


Simultaneous Detection of Herpes Simplex Virus Type 1 Latent and Lytic Transcripts in Brain Tissue

ASN Neuro
Volume 13: 1–13
© The Author(s) 2022
Article reuse guidelines:
sagepub.com/journals-permissions
DOI: 10.1177/17590914211053505
journals.sagepub.com/home/asn



Shu Zhang^{1,2} , Jianxiong Zeng^{1,2}, Yuzheng Zhou³, Ruoyun Gao³,
Stephanie Rice³, Xinying Guo^{1,2}, Yongzhen Liu³, Pinghui Feng³,
and Zhen Zhao^{1,2}

Abstract

Neurotrophic herpes simplex virus type 1 (HSV-1) establishes lifelong latent infection in humans. Accumulating studies indicate that HSV-1, a risk factor of neurodegenerative diseases, exacerbates the sporadic Alzheimer's disease (AD). The analysis of viral genetic materials via genomic sequencing and quantitative PCR (qPCR) is the current approach used for the detection of HSV-1; however, this approach is limited because of its difficulty in detecting both latent and lytic phases of the HSV-1 life cycle in infected hosts. RNAscope, a novel *in situ* RNA hybridization assay, enables visualized detection of multiple RNA targets on tissue sections. Here, we developed a fluorescent multiplex RNAscope assay in combination with immunofluorescence to detect neuronal HSV-1 transcripts in various types of mouse brain samples and human brain tissues. Specifically, the RNA probes were designed to separately recognize two transcripts in the same brain section: (1) the HSV-1 latency-associated transcript (LAT) and (2) the lytic-associated transcript, the tegument protein gene of the unique long region 37 (UL37). As a result, both LAT and UL37 signals were detectable in neurons in the hippocampus and trigeminal ganglia (TG). The quantifications of HSV-1 transcripts in the TG and CNS neurons are correlated with the viral loads during lytic and latent infection. Collectively, the development of combinational detection of neuronal HSV-1 transcripts in mouse brains can serve as a valuable tool to visualize HSV-1 infection phases in various types of samples from AD patients and facilitate our understanding of the infectious origin of neurodegeneration and dementia.

Keywords

herpes simplex virus type 1, latent infection, LAT, UL37, RNAscope

Received July 21, 2021; Revised September 22, 2021; Accepted for publication September 28, 2021

Summary Statement

To visualize the lytic and latent phase of HSV-1 in the infected neuron, a fluorescent multiplex RNAscope assay in combination with immunofluorescence was developed to detect neuronal HSV-1 transcripts in infected mouse brain tissues.

Introduction

Herpes simplex virus 1 (HSV-1), a neurotrophic human pathogen, comprises a linear double-stranded DNA genome wrapped by an icosahedral capsid, which is encircled by both tegument and viral envelope (Liu et al., 2019). After primary infection in sensory neurons, HSV-1 liberates

¹Department of Physiology and Neuroscience, University of Southern California, Los Angeles, CA, USA

²Zilkha Neurogenetic Institute, Keck School of Medicine, University of Southern California, Los Angeles, CA, USA

³Section of Infection and Immunity, Herman Ostrow School of Dentistry, Norris Comprehensive Cancer Center, University of Southern California, Los Angeles, CA, USA

Corresponding Author's:

Shu Zhang, Department of Physiology and Neuroscience, University of Southern California, Los Angeles, CA, 90033, USA.
Email: zhan799@usc.edu

Jianxiong Zeng, Department of Physiology and Neuroscience, University of Southern California, Los Angeles, CA, 90033, USA.
Email: zengj@usc.edu

Zhen Zhao, Department of Physiology and Neuroscience, University of Southern California, Los Angeles, CA, 90033, USA.
Email: zzhao@usc.edu



its DNA into the nucleus to establish latency during which the viral DNA is chromatinized and only latency-associated transcripts (LATs) and several microRNAs (miRNA) are expressed. These LATs and miRNAs cooperate closely to suppress HSV-1 propagation, inhibit host apoptosis, and contribute to the stimulation of viral reactivation (Gupta et al., 2006). The common symptom of HSV-1 infection is cold sores at the oral mucosa, while a severe form of diffused acute infection can result in a rare herpes simplex encephalitis (HSE) in the brain (Nicoll et al., 2012). Periodic reactivations of HSV-1 from latency contribute to viral spreading in the central nervous system (Doll et al., 2019; Marcocci et al., 2020). This latent inflectional spread to the brain is also supported by clinical evidence which shows HSV-1 genome detection in postmortem brain samples from patients who failed to show any clinical HSE symptoms (Baringer & Pisani, 1994; Fraser et al., 1981). HSV-1 reactivation from latency usually occurs by multiple stimuli, including repeated HSV-1 infection, physical or emotional stress, brain insults, or immunosuppression, which have been attributed to neurodegenerative diseases, such as sporadic Alzheimer's disease (AD) (Bourgade et al., 2016; Doll et al., 2019; Itzhaki et al., 2016; Kumar et al., 2016; Marcocci et al., 2020).

An increasing number of studies indicate that microbial infection accelerates the formation of amyloid-beta ($A\beta$) plaque and hyperphosphorylated tau, hall-markers of AD (Alvarez et al., 2012; Bourgade et al., 2016; Ezzat et al., 2019; Heneka et al., 2015; Itzhaki et al., 2016; Kumar et al., 2016), further implicating the causative role of HSV-1 in AD pathogenesis (Eimer et al., 2018; Ezzat et al., 2019; Readhead et al., 2018; Santana et al., 2012). However, the understanding of how HSV-1 latent infection and its reactivation promote AD progression is largely unknown. Thus, it is crucial to employ a practical and accurate detection approach of HSV-1 infection status to develop an effective disease treatment for human patients. Currently available diagnostic tools mainly rely on serological and molecular-based methods (Anderson et al., 2014), both dependent on the production of HSV-1 antibody, which can be detected by immunoassays or through a variety of standard or modified quantitative PCR. These diagnostic approaches can detect HSV-1 infection, but the detection limit, in particular for latent genes with minimum expression levels, becomes an obstacle in distinguishing phases of the HSV-1 life cycle present in brain tissues. The detection of herpesviruses in AD brains by shotgun sequencing and modified Viromescan bioinformatics analysis also raised questions on the sensitivity and specificity of the detection methods (Allnut et al., 2020; Chorlton, 2020; Readhead et al., 2018). Therefore, the development of an accurate, direct, and practical detection method to: (1) detect low levels of HSV-1 latent gene expression on time; and (2) distinguish between HSV-1 latency and reactivation in human patients is an urgent demand.

RNAscope, a type of in situ RNA hybridization assay, has been developed to meet the need for high sensitivity and

specificity (Jolly et al., 2019; Wang et al., 2012). Compared to conventional fluorescence in situ hybridization (FISH) with long probes (Cohen et al., 2020), RNAscope probes are ~20 pairs of double Z probes designed specifically for each transcript, and therefore, the signals are more specific and sensitive for the low level of transcripts in the forms of puncta. This method is particularly suitable for detecting the latency and reactivation status of HSV-1 in the brain. In addition, the most intriguing feature of the RNAscope is to simultaneously visualize the detection of multiple RNA targets on various tissue samples. The present study is the first attempt to develop the fluorescent multiplex RNAscope approach, combining immunofluorescence with neuronal markers to detect neuronal HSV-1 latent LAT and lytic UL37 transcripts in mouse brain tissues. This advanced detection method warrants the detectability of HSV-1 latent genes and enables the distinction between latency and lytic replication status at the single-cell level in brain tissues. The RNAscope-based combinational detection tool in mouse brain tissues can be applied to human brain samples for multiple diseases such as HSV-1 potentially induced neurodegeneration.

Materials and Methods

Cells and Viruses

Vero cells were maintained in Dulbecco's Modified Eagle Medium (DMEM) supplemented with 10% fetal bovine serum and 1% penicillin-streptomycin solution at 37 °C in a 5% CO₂ humidified incubator. Human herpesvirus 1 (strain 17) (HSV-1) viruses were amplified by routine propagation on Vero cell monolayer as we previously described (Zhang et al., 2018). Infected Vero cells were collected at 48 h post infection, frozen, and thawed three times in PBS. A filtered viral-containing solution was titrated by plaque assays on a Vero cell monolayer. Stocks were aliquoted and stored at -80 °C for further use.

Infection of Mice

The 5xFAD transgenic mice are commonly used mouse models to study the role of HSV-1 infection in AD as continuously reported (Eimer et al., 2018; Ezzat et al., 2019; Sait et al., 2021). To better represent the infection status of HSV-1 in the AD brain, we chose to use 5xFAD mice for the RNAscope assay. A total of 8 age- and gender-matched 5 × FAD transgenic mice (12–14 weeks old) were used for mock- ($n = 3$) and HSV-1 ($n = 5$) infection. The infection group was challenged with 5×10^5 PFU of HSV-1 via intravenous injection, a reliable HSV-1 invasion in the brain as previously reported to achieve latency in neurons (Kulu et al., 2009; Nicoll et al., 2016; Yao et al., 2014). At one- and five- weeks post infection, infected mice were euthanized, and trigeminal ganglia (TG) and brains were collected for later analysis. To represent the acute infection resulting

from HSV-1 lytic replication, mice ($n=3$) were challenged with 5×10^6 PFU of HSV-1 via intravenous injection. TGs and brains were collected at 4 days post infection.

Human Tissue

Human brain cortex samples from AD subjects were obtained from National Disease Research Interchange (NDRI), US. Fresh tissue was either stored at -80°C or fixed in 10% neutral buffered formalin for one week prior to being embedded in paraffin. Samples were further prepared according to the manufacturer's instruction (Formalin-Fixed Paraffin-Embedded (FFPE) Sample Preparation and Pretreatment, Document #322452, ACD, Inc.). Briefly, all experimental procedures were performed under relevant guidelines and regulations.

Quantification of Viral Genome and Transcripts by Real-Time PCR

Brains and TGs of infected mice were homogenized in PBS by a mini-beads beater (Biospec) and genomic DNA was extracted using the salt precipitation protocol (Chen et al., 2015), and HSV-1 genome copy numbers were determined by real-time PCR. Cycle conditions were as follows: 95°C for 10 min and 95°C for 15 s followed by 60°C for 1 min (40 cycles) (Kubat et al., 2004). Genome copies were normalized to host constitutive housekeeping genomic β -actin. Purified plasmid DNA was used for generating the standard curve. The cutoff CT value was set at 34 cycles as determined by running a series of diluted standard curves using plasmid DNA. RNA was extracted using TRIzol reagent (Invitrogen). RNA was first digested with DNase I (New England Biolabs) to remove genomic DNA. One microgram of total RNA was used for reverse transcription with RNA-dependent DNA polymerase for cDNA synthesis (Promega) according to the manufacturer's instruction. Briefly, RNA mix with 0.5 μg corresponding primers (Oligo(dT) or random primers) was incubated at 70°C for 5 min followed by incubation at 4°C for 5 min. A reverse transcriptase reaction mix (15 μL per reaction) was added to the RNA mix for incubation at 25°C for 5 min and 42°C for 60 min. Approximately 10 ng of the cDNA was used as a template in each quantitative real-time PCR (qRT-PCR) reaction with SYBR master mix (Applied Biosystems). Primers for qRT-PCR are included in Table 1.

RNAscope In-Situ Hybridization

To examine HSV-1 mRNA on different types of samples, RNAscope was performed on fixed frozen tissue sections (mouse tissue) and FFPE-fixed brain slices (mouse and human tissues). To prepare fixed frozen slides, mouse brains were perfused with PBS-1% EDTA buffer and fixed in 4% paraformaldehyde overnight at 4°C in the dark. Fixed tissues were dehydrated by sequentially merging in 10% and 30% sucrose solutions (Grabinski et al., 2015), followed by freezing in O.C.T. at -80°C . Sections of 10 μm were cut from frozen biopsies, dried for 10 min at RT for further processes, and 8 μm sections were cut from FFPE blocks. In situ hybridization (ISH) was performed according to the detection protocols (details are included below), RNAscope Multiplex Fluorescent Reagent Kit v2 (ACD, Inc, Cat. No. 323100) and RNAscope 2.5 HD Detection Reagent Kit (ACD, Inc, Cat. No. 322360) with modifications of IF staining protocol.

Briefly, slides from fixed frozen brains were dried in an oven at 60°C for 30 min prior to incubation in cold 4% PFA for 15 min. RNase control slides were incubated with 100 $\mu\text{g}/\text{mL}$ RNase (Sigma) for 30 min at 30°C . Slides were washed with PBS buffer twice and dehydrated in 50%, 70%, and 100% ethanol for 5 min each at room temperature (RT). H_2O_2 (provided by the manufacturer) was added to the air-dried samples for 10 min at RT. Slides were washed with distilled water twice and treated with protease IV (provided by the manufacture) for 30 min at RT. For combined ISH and IF treatment, prior to the fixation and ethanol dehydration for RNAscope pretreatment, frozen brain sections were first stained with primary antibody overnight, e.g., anti-NeuN antibody (1:200 dilution; Abcam, ab177487), followed by the secondary antibody to confirm the staining. Notably, to enhance the quality of IF staining, re-probing with anti-NeuN antibody and secondary antibody following RNAscope assay is recommended.

For FFPE-fixed sections, slides were baked at 60°C for 1 h before deparaffination in xylene and 100% ethanol, 5 min each at RT. H_2O_2 was added to the air-dried samples for 10 min at RT. For antigen retrieval, slides were incubated in the boiling antigen retrieval buffer ($>98^\circ\text{C}$) for 15 min, washed in distilled water twice, then dehydrated in 100% ethanol. Protease Plus was added to the samples for 40 min at 40°C in the HybEZ oven.

RNAscope assays were performed on pretreated samples according to the manufacturer's instructions. In summary, pretreated slides were incubated with probe mixtures for 2 h at 40°C . C1 probes were designates for HSV-1 UL37

Table 1. Primers of Interested Genes for RT-PCR.

Gene Target	Forward (5'-3')	Reverse (5'-3')
β -actin	TCTACGAGGGCTATGCTCTCC	TCTTTGATGTCACGCACGATTTCC
UL37	GGAGCTGTACGTGATCTCCA	CCAGGGCGTACATGCTAATC
LAT	GGCCGGTGTGCTGTAAC	CCAGGCAGTAAGACCCAAGC

mRNA (customized probes, targeting the region 1,793- 3,332 bp of UL37 mRNA) (Cat # 892001; ACD. Inc), detected with Opal 520 fluorophore. C2 probes were assigned for HSV-1 LAT mRNA (Probe - HSV-1-LAT, Cat # 315651; ACD. Inc), targeting the region from 118,806 bp to 125,028 bp of LAT, which covers the stable 2.0-kb intron region (Jaber et al., 2009). C2 probes were detected with Opal 570 fluorophore. C3 probes (Cat # 431158; ACD. Inc) were set to *Map2* mRNA and detected with Opal 690 fluorophore. Each probe contains 36 to 50 bases. After probe hybridization, slides were washed twice using wash the buffer provided in the kit. The preamplification step was performed to allow binding of preamplification probe to RNAScope probes. The second and third amplification steps were conducted by incubating slides with amplification buffer containing excessive amplifiers which bind to the multiple binding sites on each preamplifier. All three amplification steps were performed at 40 °C for 30 min followed by washing twice with wash buffer. To develop a fluorescent signal for probe C1, HRP solution was added to the section for 15 min at 40 °C. After 2 min washing, the section was probed with opal dye for 30 min at 40 °C, followed by the HRP blocker for 15 min at 40 °C. This process was repeated for the fluorescence development for probes C2 and C3. Lastly, DAPI was added to the section for nucleus staining prior to mounting the slide. For IF with anti-NeuN marker, Alexa 647 secondary antibodies were used. Positive probe (Mouse *PP1B*; Cat # 313911; ACD. Inc), encoding peptidyl-prolyl cis-trans isomerase B, is a housekeeping gene. *Ppib* has been recognized as a common reference gene for RT-PCR normalization (Bruckert et al., 2016) and a technical assay control for RNAScope. *Escherichia coli DapB* serves as a negative probe (Cat # 310043; ACD. Inc).

Confocal Imaging

Tissue sections were evaluated and captured under an inverted confocal microscope (Nikon Eclipse Ti2) at 10–60×

objective. Imaging settings were adjusted based on the positive and negative controls. The negative control slide was assessed first to eliminate the imaging background. The positive control slide was assessed to determine the signal strength. To increase the sensitivity for detecting HSV-1 mRNA signals, 60× objective was used to better visualize the images. Fiji software was used for particle analysis and auto-segmentation process.

Results

Limitation of HSV-1 Detection via RT-PCR in Tissue Samples

The most common form of HSV-1 infection in the human population is latent infection. To establish the latent infection model in mice and study its role in the diseased condition, we infected $5 \times \text{FAD}$ transgenic mice (12–14 weeks old) with 5×10^5 PFU of HSV-1 via intravenous injection. Hunched postures and paralysis were observed at 5–7 days post infection, which is likely because of the lytic replication of HSV-1 in the nervous system (Doll et al., 2019). However, the infected mice soon recovered and showed no such signs at five weeks post infection (data not shown). After one week of acute infection, we detected approximately 1.7×10^4 genome copies of HSV-1 per million actin copies in 10 ng total DNA from infected mouse brains (Figure 1A). The presence of high HSV-1 DNA load demonstrates the successful invasion of HSV-1 in the mouse brain. At five-week post infection, the viral genome load reduced by 8-fold to 2.1×10^3 copies (Figure 1A), suggesting an overall transition from lytic replication to latency regarding HSV-1 infection status.

To further validate the latent and lytic status of HSV-1 infection, we extracted the total RNA from the mouse brain and performed Reverse-Transcription PCR (RT-PCR) to quantify the LAT and UL37 transcripts, respectively. Unfortunately, the levels of both transcripts were close to

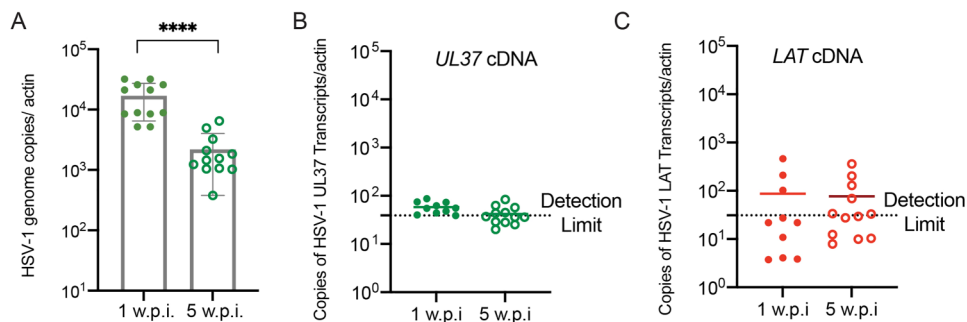


Figure 1. RT-PCR has limitations in detecting HSV-1 transcripts in mouse brains. (A) Genome copies of HSV-1 in the infected mouse brains at one- and five-weeks post infection (w.p.i). A total of 10 ng DNA was used for real-time RCR quantification. Genome copies were normalized to host constitutive housekeeping genomic β -actin ($\times 10^6$). The cutoff CT value was set at 34 cycles as determined by running a series of diluted standard curves using plasmid DNA. **** $P < .001$ were calculated by Student's *t* test. (B) UL37 and (C) LAT transcripts in the infected mouse brain at one and five w.p.i.

the detection limits (Figure 1B and C). Such detection limits of the HSV-1 transcripts in infected mouse brains were consistently observed in previous studies (Kelly et al., 2008; Menendez & Carr, 2017). Therefore, it is important to develop a better quantitative detection means to directly reveal the status of HSV-1 infection.

RNAscope Assay Detects HSV-1 mRNA in Mouse and Human Brain Tissues

RNAscope assay (Figure 2A) has been applied as a semiquantitative tool for infectious diseases, including human papillomavirus (HPV) infection in human head and neck cancer, and Epstein-Barr virus (EBV) infection (Cimino et al., 2014; Ukpo et al., 2011; Wang et al., 2012). To test the RNAscope-based detection for HSV-1, we first examined the specificity and sensitivity of the probes targeting HSV-1 UL37 or LAT on mouse frozen brain sections. Positive and negative controls were used for image acquiring settings as described in the Methods and Materials (Figure 2B). As such, the signal for neither UL37 nor LAT transcripts was observed in mock-infected samples (Figure 2B) or the RNAse control (Figure 2C).

In the hippocampus of the HSV-1 infected mice (Figure 2D), we observed green and red puncta representing the mRNA signals of UL37 and LAT, respectively. Interestingly, three types of infected cells can be observed: (1) UL37 positive (17.3%), (2) LAT positive (46.4%), and (3) UL37 and LAT double-positive cells (13.1%) per total cells (Figure 2G), indicating the different infection stages of HSV-1 (lytic active, latent, and transition between lytic and latent stages). Average numbers of LAT and UL37 puncta in each infected cell are calculated as 3.5 and 2.8, respectively (Figure 2H), suggesting the heterogeneity of HSV-1 infection status in the brain, which could not be reflected by the traditional diagnostic methods. The colocalization of LAT transcripts and UL37 transcripts is observed, suggesting the formation of stress granules and perhaps the low level of spontaneous reactivation of HSV-1 as previously reported (Wilson & Mohr, 2012). This suggestion is also supported by the fact that HSV-1 is capable of regulating stress granule formation in the infected host (Gaete-Argel et al., 2019). The ability to detect both transcripts is a valuable strength of the current multiplex approach, compared to conventional RNA-DNA FISH which detects LAT alone, or immunostainings which can only recognize viral antigens.

To further validate this RNAscope detection approach, we performed an HSV-1 acute infection on 5xFAD and WT mice (Figure 3 and Figure S1). Besides the brain collection, TGs were also collected at 4 days post infection since the sensory neurons of TGs are the primary infection site of HSV-1 (Figure 3A). The level of viral transcripts during acute infection is much higher than that during latency, indicating the active lytic replication of HSV-1 (Figure 3B and C),

particularly in TGs. The viral loads based on genome copies in extracted tissues showed a more than 10-fold reduction in HSV-1 level in both the TG and brain during latency (Figure 3D) when compared to the acute phase, which is largely consistent with previous observations (Cherpes et al., 2008; Li et al., 2020; Rock & Fraser, 1983). Based on RNAscope analysis, there was nearly a 3-fold reduction in the number or percentage of neurons carrying HSV-1 UL37 and/or LAT transcripts in latency (37.3%) (Figure 3E), as well as a 2-fold reduction in an average number of puncta (2.3 per cell) in neurons carrying HSV-1 transcripts (Figure 3F), indicating that the RNAscope analysis is reflecting the genome quantification data. Similar results were obtained from RNAscope analysis of the infected TG, which is consistent with previous findings (Burgos et al., 2005; Menendez et al., 2016). HSV-1 infected TG exhibits neuron-to-neuron heterogeneity (Mehta et al., 1995) in that some neurons harvest much more signals of HSV-1 transcripts than others during acute infection, but the average numbers of puncta per HSV-1 positive cells are still comparable to that in the hippocampus. Yet, the spatial resolution and sensitivity, particularly in detecting latent transcripts, can only be obtained using RNAscope. These findings also provide a valuable reference for future HSV-1 detection in related studies.

We also validated the probes on the mouse and human FFPE samples using the RNAscope chromogenic detection kit. The mouse FFPE samples were collected at one week post infection and the low level of LAT signals could be observed (Figure 4A), indicating the high sensitivity of the RNAscope assay. As for human brain tissue sections, we also successfully detected the LAT mRNA signals from four cortex samples infected with HSV-1 (Figure 4B and Figure S2), but not in HSV-1 negative samples (Figure 4C). More LAT signals can be observed in the sample with a higher viral load (Figure 4B and Figure S2A). Our results above suggest the feasibility of applying the RNAscope approach for the detection of HSV-1 infection in humans.

Combining RNAscope and Immunofluorescence to Specify HSV-1 Infected Neurons

To further identify the cell type infected by HSV-1, we applied a combined RNAscope and immunofluorescence approach to simultaneously visualize the mRNA signals and cell markers. As a neurotrophic virus, HSV-1 primarily targets neurons. Hence, we selected two neuronal markers, *Map2* by RNAscope and NeuN by immunofluorescence, for neuron identification (Table 2). Both *Map2* RNAscope probe and anti-NeuN antibody successfully recognized neurons in the mouse hippocampus (Figure 5A and B). Compared to the *Map2* probe, combined RNAscope and immunofluorescence with anti-NeuN antibody staining

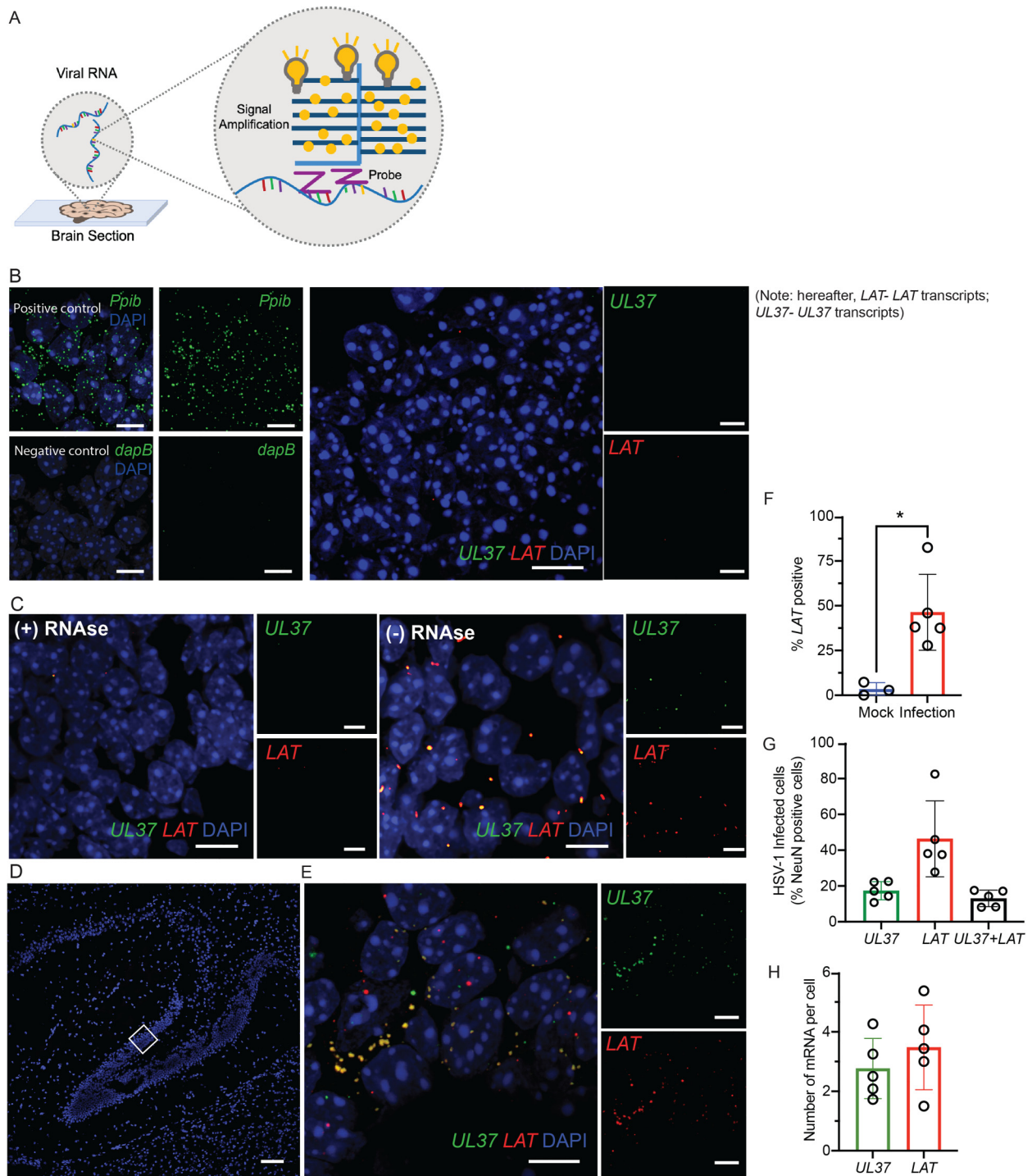


Figure 2. RNAscope assay enables the detection of HSV-1 mRNA on mouse fixed frozen samples. (A) Illustration of RNAscope working mechanism. (B) Positive control and negative control (left), and mock control (right). (C) RNase treated control to digest RNA (left panel) and nontreated (right panels) control. UL37 and LAT mRNA in mock (B) and HSV-1 infected (D-E) mouse brains at five w.p.i. by RNAscope detection. (F) Quantification of mRNA signals in mock and HSV-1 infected sections. % LAT positive cells per image. * $P < .05$ were calculated by Student's *t* test. (G) Numbers of LAT and/or UL37 positive cells. (H) Average number of LAT and UL37 mRNA per cells. Error bars represent standard deviations (SD). Scale bar = 100 μ m in (D) and 10 μ m in (A, B, C, E).

exhibited much distinct and stronger signals, which can be applied to the fragmented individual cells for further quantification analysis.

Interestingly, the activities of HSV-1 transcription were divergent in Dentate Gyrus (DG) and Cornu Ammonis (CA) regions in the hippocampus (Figure 5B). For example, UL37

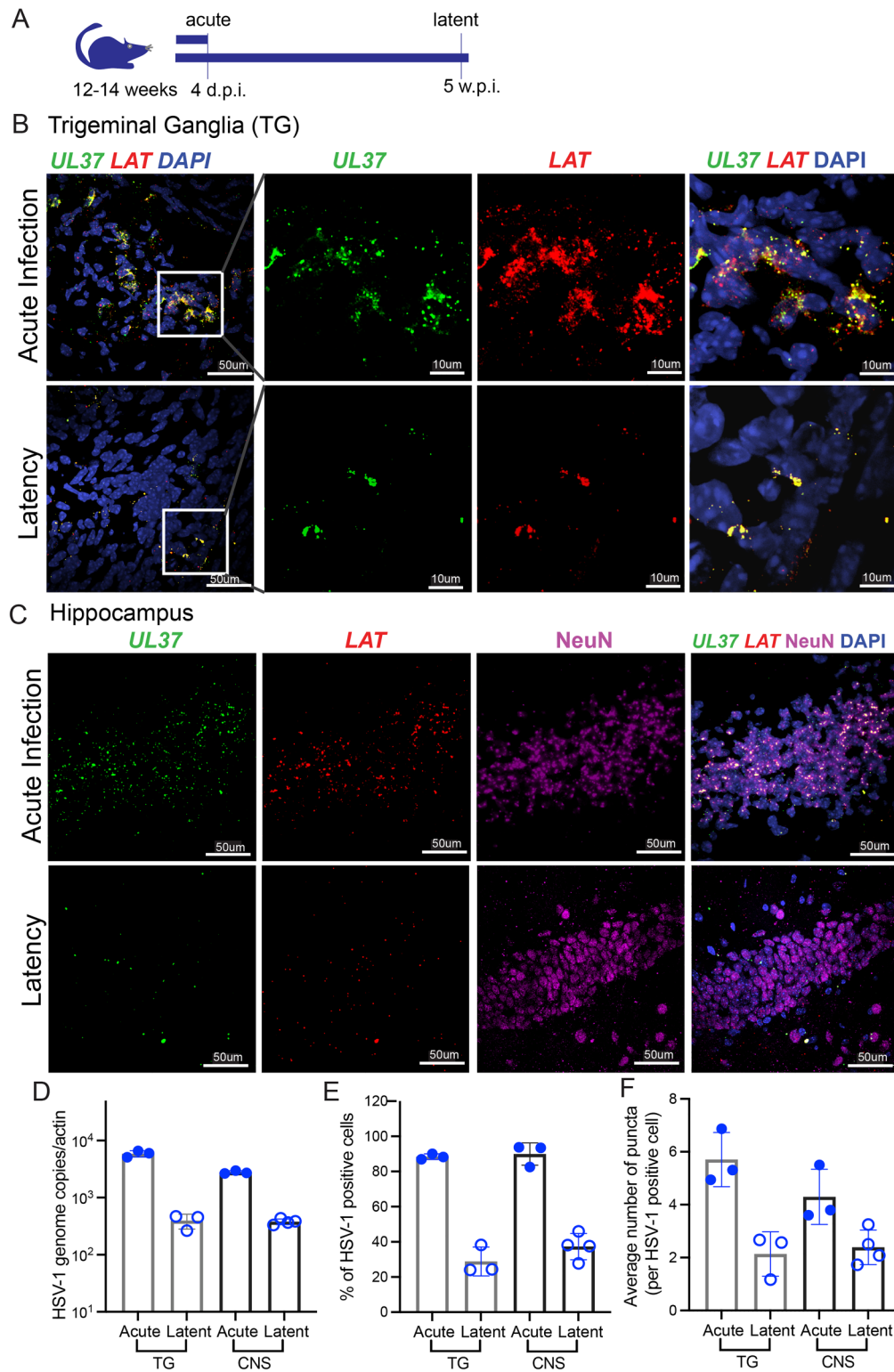


Figure 3. RNAscope analysis detects HSV-1 on acutely and latently infected mouse tissues. (A) Illustration of HSV-1 acute and latent infection models. (B) Detection of UL37 and LAT mRNA in trigeminal ganglia of HSV-1 infected mouse. (C) UL37 and LAT mRNA in *Map2* and NeuN positive cells in the mouse brains infected with HSV-1. (D) Quantification of HSV-1 genomes. (E) Quantification of HSV-1 infected neurons, containing either of both LAT and UL37. (F) Number of puncta per HSV-1 positive cell in the acutely and latently infected mouse brains. Cell number and puncta were analyzed using Fiji, the function of analyze particle. Average number of puncta per HSV-1 positive cells was calculated using the total number of puncta divided by the number of HSV-1 positive cells per image. One section per mouse was used for quantification, $n = 3$ or 4. Scale bars are included with indicated values.

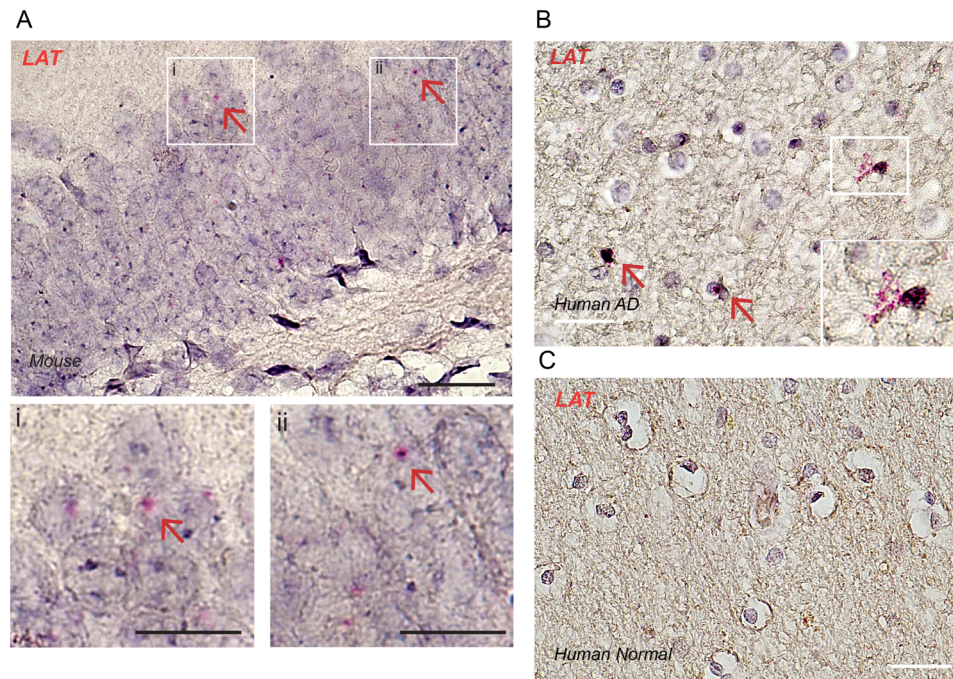


Figure 4. Detection of HSV-I mRNA using FFPE samples. (A) LAT mRNA in the infected mouse brain. C57BL/6J mouse was infected with 5×10^6 HSV-I via intravenous injection. The brain was collected at 5 days post infection. (B) LAT mRNA in AD patient brain tissue section (ID number is 877. Additional information of donor is listed in Figure S2A). (C) LAT mRNA in normal brain tissue section (ID number is ND12975). Scale bar = 20 μ m; 10 μ m for magnification images i) and ii).

Table 2. Combined RNAscope and/or Immunohistochemistry Staining on Brain Tissues.

RNAscope targeted transcript	IHC targeted cell marker	RNAscope targeted cell marker	Organ	Tissue sample type	Reference
<i>SNAP25</i>		<i>Map2</i>	Human brain	FFPE	(Jolly et al., 2019)
<i>ApoE</i>		<i>Itgam</i>	Mouse brain	Fresh frozen	(Sala Frigerio et al., 2019)
<i>Cd22</i>		<i>Tmem119</i>	Mouse brain	Fresh frozen	(Pluvinage et al., 2019)
<i>Tlr7</i>		<i>Tmem119</i>	Mouse brain	Fresh frozen	(Michaelis et al., 2019)
<i>MS4A7</i>	Iba1	<i>Tmem119</i>	Human brain	FFPE	(Bennett et al., 2018)
<i>Vtn</i> or <i>Iftm1</i>		<i>Pdgfra</i>	Mouse brain	Fresh frozen	(He et al., 2016)
<i>Ccl5</i>	NeuN		Rat brain	Fixed frozen	(Lanfranco et al., 2018)
<i>Ccl5</i>	GFAP				
<i>Ccl5</i>	Iba1				
<i>Ccl5</i>	Nkx2.2				

FFPE: Formalin-fixed paraffin-embedded.

IHC: Immunohistochemistry.

Neuron marker: *Map2*, NeuN.

Microglia marker: *Tmem119*, Iba1, *Itgam*.

Astrocyte marker: GFAP.

Pericyte marker: *Pdgfra*.

Oligodendrocyte progenitor marker: *Nkx2.2*.

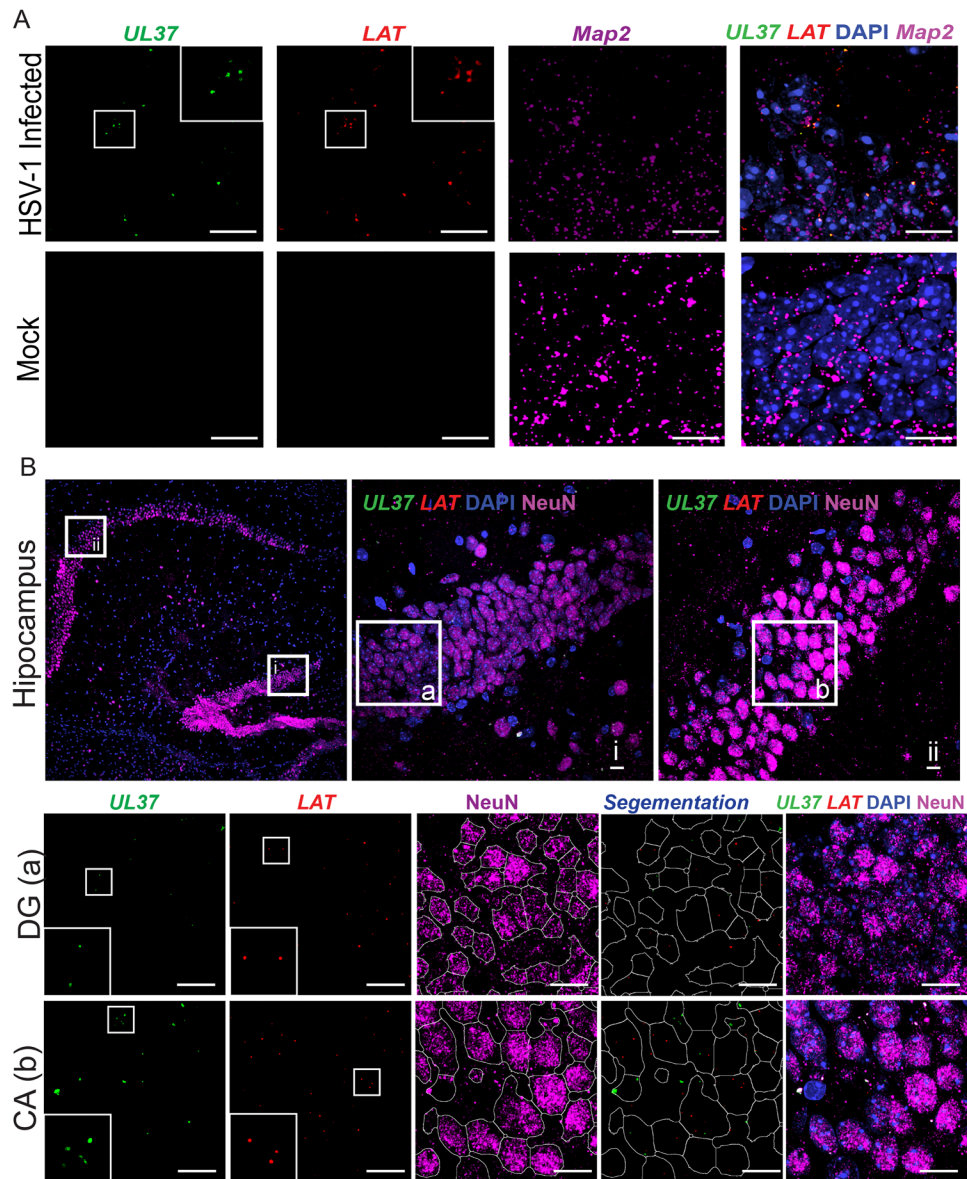


Figure 5. RNAscope multiplex fluorescent assay to detect HSV-1 mRNA in labeled neurons. (A) UL37 and LAT mRNA in *Map2* positive cells in mock and HSV-1 infected mouse brains. (B) UL37 and LAT mRNA in NeuN positive cells in mouse hippocampus. Fiji software was used for particle analysis and auto-segmentation process. Scale bar = 10 μ m.

transcription was much more active in CA neurons compared to DG neurons. A recent study on neuronal vulnerability in AD indicates that different neuronal cells display different levels of vulnerabilities contributing to AD pathogenesis (Roussarie et al., 2020). Specifically, in terms of gene regulation of β -amyloid aggregation and neurofibrillary tangles, CA1 neurons were characterized as vulnerable cells, while DG neurons were characterized as resistant.

Discussion

Herpesviruses are ubiquitous human pathogens and are recognized as emerging risk factors underpinning diverse chronic

diseased conditions, including atherosclerosis and neurodegeneration (McQuillan et al., 2018). Recent studies estimate that in the US, the percentage of humans infected with HSV-1 increases consistently with age from 47.8% in adults (14–49 years) to 65% among those >70 years old (McQuillan et al., 2018; Xu et al., 2002). Periodic reactivation and replication of HSV-1 in elders can increase the risk of neuroinflammation, neuronal damage, and cognitive impairment, predisposing the brain to AD (Katan et al., 2013; McManus & Heneka, 2017). Given the prevalence of HSV-1 infection in the general population, the clinical diagnosis of HSV-1 has been developed for a long time. To our best knowledge, molecular- and serological-based assays are

the major methods for clinical HSV-1 diagnosis (Anderson et al., 2014). However, these commonly used assays have limitations in detecting low levels of HSV-1 transcripts in the infected host. Although the low level of gene expression can be achieved by RNAseq and the existence of HSV-1 in AD have been recently confirmed (Roussarie et al., 2020), only a handful of reads can be mapped to the HSV-1 genome. This is caused by a very low level of HSV-1 transcription in only a small set of cells in the brain and the abundance of these transcripts is incomparable to endogenous genes. The low copies of HSV-1 transcripts in a given single cell may not be significant; it has been shown both clinically and preclinically that HSV-1 latency is common in our general population without causing detrimental consequences in brain health (Readhead et al., 2018). However, both HSV-1 latent transcripts have been shown to have a much broader influence on the epigenetic regulation and posttranslational modification of host cells, which has become more widely recognized. More importantly, local reactivation in the brain may act as a trigger for neurodegenerative or pathological cascades, e.g., the seeding of amyloid (De Chiara et al., 2010). Therefore, we developed the HSV-1 detection method with high sensitivity and specificity based on the RNAscope technology, which enables the direct detection of low-expressed multiple HSV-1 latent or lytic transcripts in infected brains, providing a better and in-depth understanding of the infectious origin of neurodegeneration.

Both serological and molecular-based methods have been commonly utilized to perform clinical HSV-1 diagnosis (Anderson et al., 2014). A serology-based method, an HSV-1 antibody-dependent immunoassay, mainly includes whole-antigen- and IgG-based detection tools; the latter is a relatively newer one to fulfill HSV type-specific diagnosis. While it is of value primarily in the determination of post exposure to HSV-1 and prenatal screening, the sensitivity of the serological assay is potentially affected by the timing after HSV-1 primary infection. So far, multiple molecular tests have been developed based on principal amplification and detection of HSV-1 viral genome target (Reil et al., 2008; Tong et al., 2012). Notably, the three tests including the PCR-based MultiCode-RTx, HSV Q^x, and IsoAmp HSV are FDA-approved for HSV-1 or -2 in a variety of swab samples (Anderson et al., 2014). Specifically, the sensitivity of PCR is capable of detecting HSV-1 genomic DNA, which is enough to diagnose the HSV-1 existence in clinical samples. But it is usually difficult to quantitatively detect either HSV-1 latent or lytic transcripts in human or mouse tissues. For example, the RT-PCR that we employed in the present study failed to detect the transcripts of both the LAT, a latent gene, and the UL37, a lytic gene in HSV-1 infected mouse brains (Figure 1C and D). Given that cellular HSV-1 infection status is the result of delicate regulation between the virus and the host, both latency and reactivation statuses are likely to co-exist in different or even the same neural cell. Unfortunately, both serological or molecular-

based methods fail to achieve more accurate diagnostic purposes such as simultaneous detection of latent and lytic genes in clinical samples. The RNAscope-based assay with high sensitivity and specificity applied in this study enables simultaneous, visualized detection of multiple RNA targets on mouse tissue sectioning (Figure 2 and 4). Specifically, the LAT and UL37 signals were detectable in different or even the same neuronal cell mostly in the hippocampus (Figure 5), demonstrating heterogeneity of HSV-1 infection status in the brain. Importantly, we developed a fluorescent multiplex RNAscope in combination with immunofluorescence to detect neuronal HSV-1 transcripts in the brains of mouse models, which can be extended to detect multiple HSV-1 transcripts in different cell types, such as microglia (IHC marker: TMEM119, Iba1), pericyte (IHC marker: PDGFRB), and astrocytes (GFAP) (Table 2). The developed RNAscope-based assay can be potentially applied in detecting HSV-1 in cultured cells and brain cell-specific HSV-1 latent and/or lytic infection in tissues.

The property of the lifelong latent infection and the existence of the latency-to-reactivation phases is the basis for the hypothesis that HSV-1 reactivation is causally linked to aging-associated diseases, including neurodegenerative AD. The interior complexity on both aspects of virus neuroinfection and host immuno-regulation contributes to the existence of the neural cell- or the phase-specific regulatory mechanisms in HSV-1 infected brains. The developed RNAscope assay can be applied to simultaneously detect HSV-1 latent/lytic genes and other AD-related targets in specific brain cells when combined with cell markers in the brain sections of laboratory mouse models or AD patients. Such a combinational assay helps to understand neural cells- or the HSV-1 infection phase-specific mechanisms underlying AD pathogenesis. In addition, delicate quantification of HSV-1 latent and lytic transcripts in specific brain cell types should be further explored with the developed RNAscope assay, which is useful in understanding the correlation between the HSV-1 infection phase and the disease progression of AD.

Conclusive Remarks

The association between infectious agents and AD has been greatly recognized; however, the mechanistic understanding is largely unknown. The different infection statuses of the microbes, such as the latency and lytic replication of HSV-1, further complicate the pathogenesis of AD promoted by microbial pathogens. The development of a practical and sensitive detection assay can provide the valuable reference necessary to determine accurate infection phases and appropriate therapeutic approaches. We applied a modified RNAscope assay to quantitatively detect latent and lytic infected HSV-1 in AD mouse brains. The successful utilization of this detection assay will ensure the identification of pathogen specificity for other neurodegenerative disorders.

Animal Protocol

All animal procedures were conducted in strict accordance with the recommendation in the Guide for the Care and Use of Laboratory Animals of the National Institutes of Health. The experimental protocol was approved by the Institutional Animal Care and Use Committee (IACUC) of the University of Southern California.

Acknowledgments

We would like to thank Dr. Weiming Yuan, Molecular Microbiology and Immunology, Keck School of Medicine of USC for providing HSV-1. We also thank the help of Ali Can Savas for the animal work.

Author Contributions

Z.Z., S.Z., and J.Z. conceived the research and designed the study. S.Z. and J.Z. wrote the manuscript. S.Z. analyzed the data. S.Z., Y.Z., R.G., S.R., Y.L., and X.G. performed the experiments. P.F. gave insightful criticism on the manuscript. All authors commented on the manuscript.

Ethics Statement

All animal procedures were conducted in strict accordance with the recommendation in the Guide for the Care and Use of Laboratory Animals of the National Institutes of Health. The experimental protocol was approved by the Institutional Animal Care and Use Committee (IACUC) of the University of Southern California. Human brain cortex samples from AD subjects were obtained from National Disease Research Interchange (NDRI), US.

Declaration of Conflicting Interests

The author(s) declared no potential conflicts of interest with respect to the research, authorship, and/or publication of this article.

Funding

The author(s) disclosed receipt of the following financial support for the research, authorship, and/or publication of this article: This work was supported by the National Institutes of Health (grant number R35DE027556, R01CA221521, R01DE026003, R03AG063287, R21AG066090, R01NS110687).

ORCID iD

Shu Zhang  <https://orcid.org/0000-0002-5372-4497>

Supplemental material

Supplemental material for this article is available online.

References

- Allnutt, M. A., Johnson, K., Bennett, D. A., Connor, S. M., Troncoso, J. C., Pletnikova, O., Albert, M. S., Resnick, S. M., Scholz, S. W., De Jager, P. L., & Jacobson, S. (2020). Human herpesvirus 6 detection in Alzheimer's disease cases and controls across multiple cohorts. *Neuron*, *105* (6), 1027–1035 e1022. doi:10.1016/j.neuron.2019.12.031
- Alvarez, G., Aldudo, J., Alonso, M., Santana, S., & Valdivieso, F. (2012). Herpes simplex virus type 1 induces nuclear accumulation of hyperphosphorylated tau in neuronal cells. *Journal of Neuroscience Research*, *90* (5), 1020–1029.
- Anderson, N. W., Buchan, B. W., & Ledebroer, N. A. (2014). Light microscopy, culture, molecular, and serologic methods for detection of herpes simplex virus. *Journal of Clinical Microbiology*, *52* (1), 2–8. doi:10.1128/JCM.01966-13
- Baringer, J. R., & Pisani, P. (1994). Herpes simplex virus genomes in human nervous system tissue analyzed by polymerase chain reaction. *Annals of Neurology*, *36* (6), 823–829. doi:10.1002/ana.410360605
- Bennett, F. C., Bennett, M. L., Yaqoob, F., Mulinyawe, S. B., Grant, G. A., Hayden Gephart, M., Plowey, E. D., & Barres, B. A. (2018). A combination of ontogeny and CNS environment establishes microglial identity. *Neuron*, *98* (6), 1170.
- Bourgade, K., Dupuis, G., Frost, E. H., & Fulop, T. (2016). Anti-Viral properties of amyloid-beta peptides. *Journal of Alzheimer's Disease*, *54* (3), 859–878. doi:10.3233/JAD-160517
- Bruckert, G., Vivien, D., Docagne, F., & Roussel, B. D. (2016). Normalization of reverse transcription quantitative PCR data during ageing in distinct cerebral structures. *Molecular Neurobiology*, *53* (3), 1540–1550. doi:10.1007/s12035-015-9114-5
- Burgos, J. S., Ramirez, C., Sastre, I., Alfaro, J. M., & Valdivieso, F. (2005). Herpes simplex virus type 1 infection via the bloodstream with apolipoprotein E dependence in the gonads is influenced by gender. *Journal of Virology*, *79* (3), 1605–1612. doi:10.1128/JVI.79.3.1605-1612.2005
- Chen, S., Sanjana, N. E., Zheng, K., Shalem, O., Lee, K., Shi, X., Scott, D. A., Song, J., Pan, J. Q., Weissleder, R., Lee, H., Zhang, F., & Sharp, P. A. (2015). Genome-wide CRISPR screen in a mouse model of tumor growth and metastasis. *Cell*, *160* (6), 1246–1260. doi:10.1016/j.cell.2015.02.038
- Cherpes, T. L., Busch, J. L., Sheridan, B. S., Harvey, S. A., & Hendricks, R. L. (2008). Medroxyprogesterone acetate inhibits CD8+T cell viral-specific effector function and induces herpes simplex virus type 1 reactivation. *Journal of Immunology*, *181* (2), 969–975. doi:10.4049/jimmunol.181.2.969
- Chorlton, S. D. (2020). Reanalysis of Alzheimer's brain sequencing data reveals absence of purported HHV6A and HHV7. *Journal of Bioinformatics and Computational Biology*, *18* (3), 2050012. doi:10.1142/S0219720020500122
- Cimino, P. J., Zhao, G., Wang, D., Sehn, J. K., Lewis, J. S., Jr., & Duncavage, E. J. (2014). Detection of viral pathogens in high grade gliomas from unmapped next-generation sequencing data. *Experimental and Molecular Pathology*, *96* (3), 310–315.
- Cohen, C., Corpet, A., Maroui, M. A., Juillard, F., & Lomonte, P. (2020). Latent/quiescent herpes simplex virus 1 genome detection by fluorescence in situ hybridization (FISH). *Methods in Molecular Biology*, *2060*, 185–197. doi:10.1007/978-1-4939-9814-2_10
- De Chiara, G., Marocci, M. E., Civitelli, L., Argnani, R., Piacentini, R., Ripoli, C., Manservigi, R., Grassi, C., Garaci, E., & Palamara, A. T. (2010). APP Processing induced by herpes simplex virus type 1 (HSV-1) yields several APP fragments in human and rat neuronal cells. *PLoS One*, *5* (11), e13989.
- Doll, J. R., Thompson, R. L., & Sawtell, N. M. (2019). Infectious herpes Simplex virus in the brain stem Is correlated with reactivation in the trigeminal ganglia. *Journal of Virology*, *93* (8), e02209-18. doi:10.1128/JVI.02209-18

- Eimer, W. A., Vijaya Kumar, D. K., Navalpur Shanmugam, N. K., Rodriguez, A. S., Mitchell, T., Washicosky, K. J., György, B., Breakefield, X. O., Tanzi, R. E., & Moir, R. D. (2018). Alzheimer's disease-associated β -amyloid is rapidly seeded by herpes viridae to protect against brain infection. *Neuron*, *99* (1), 56–63.e53. doi:10.1016/j.neuron.2018.06.030
- Ezzat, K., Pernemalm, M., Pålsson, S., Roberts, T. C., Järver, P., Dondalska, A., Bestas, B., Sobkowiak, M. J., Levänen, B., Sköld, M., Thompson, E. A., Saher, O., Kari, O. K., Lajunen, T., Sverremark Ekström, E., Nilsson, C., Ishchenko, Y., Malm, T., Wood, M. J. A., ..., & El Andaloussi, S. (2019). The viral protein corona directs viral pathogenesis and amyloid aggregation. *Nature Communications*, *10* (1), 2331. doi:10.1038/s41467-019-10192-2
- Fraser, N. W., Lawrence, W. C., Wroblewska, Z., Gilden, D. H., & Koprowski, H. (1981). Herpes simplex type 1 DNA in human brain tissue. *Proceedings of the National Academy of Sciences of the United States of America*, *78* (10), 6461–6465. doi:10.1073/pnas.78.10.6461
- Gaete-Argel, A., Marquez, C. L., Barriga, G. P., Soto-Rifo, R., & Valiente-Echeverria, F. (2019). Strategies for success. Viral infections and membraneless organelles. *Frontiers in Cellular and Infection Microbiology*, *9*, 336. doi:10.3389/fcimb.2019.00336
- Grabinski, T. M., Kneynsberg, A., Manfredsson, F. P., & Kanaan, N. M. (2015). A method for combining RNAscope in situ hybridization with immunohistochemistry in thick free-floating brain sections and primary neuronal cultures. *PLoS One*, *10* (3), e0120120.
- Gupta, A., Gartner, J. J., Sethupathy, P., Hatzigeorgiou, A. G., & Fraser, N. W. (2006). Anti-apoptotic function of a microRNA encoded by the HSV-1 latency-associated transcript. *Nature*, *442* (7098), 82–85. doi:10.1038/nature04836
- He, L., Vanlandewijck, M., Raschperger, E., Andaloussi Mae, M., Jung, B., Lebouvier, T., Ando, K., Hofmann, J., Keller, A., & Betscholtz, C. (2016). Analysis of the brain mural cell transcriptome. *Scientific Reports*, *6*, 35108. doi:10.1038/srep35108
- Heneka, M. T., Carson, M. J., Khoury, J. E., Landreth, G. E., Brosseron, F., Feinstein, D. L., Jacobs, A. H., Wyss-Coray, T., Vitorica, J., Ransohoff, R. M., Herrup, K., Frautschy, S. A., Finsen, B., Brown, G. C., Verkhratsky, A., Yamanaka, K., Koistinaho, J., Latz, E., Halle, A., ..., & Kummer, M. P. (2015). Neuroinflammation in Alzheimer's disease. *The Lancet Neurology*, *14* (4), 388–405. doi:10.1016/S1474-4422(15)70016-5
- Itzhaki, R. F., Lathe, R., Balin, B. J., Ball, M. J., Bearer, E. L., Braak, H., Bullido, M. J., Carter, C., Clerici, M., Cosby, S. L., Del Tredici, K., Field, H., Fulop, T., Grassi, C., Griffin, W. S., Haas, J., Hudson, A. P., Kamer, A. R., Kell, D. B., ..., & Whittum-Hudson, J. A. (2016). Microbes and Alzheimer's disease. *Journal of Alzheimer's Disease*, *51* (4), 979–984. doi:10.3233/JAD-160152
- Jaber, T., Henderson, G., Li, S., Perng, G. C., Carpenter, D., Wechsler, S. L., & Jones, C. (2009). Identification of a novel herpes simplex virus type 1 transcript and protein (AL3) expressed during latency. *Journal of General Virology*, *90* (10), 2342–2352.
- Jolly, S., Lang, V., Koelzer, V. H., Sala Frigerio, C., Magno, L., Salinas, P. C., Whiting, P., & Palomer, E. (2019). Single-Cell quantification of mRNA expression in The human brain. *Scientific Reports*, *9* (1), 12353.
- Katan, M., Moon, Y. P., Paik, M. C., Sacco, R. L., Wright, C. B., & Elkind, M. S. (2013). Infectious burden and cognitive function: The northern Manhattan study. *Neurology*, *80* (13), 1209–1215.
- Kelly, K., Brader, P., Rein, A., Shah, J. P., Fong, Y., & Gil, Z. (2008). Attenuated multimitated herpes simplex virus-1 effectively treats prostate carcinomas with neural invasion while preserving nerve function. *FASEB Journal*, *22* (6), 1839–1848. doi:10.1096/fj.07-097808
- Kubat, N. J., Amelio, A. L., Giordani, N. V., & Bloom, D. C. (2004). The herpes simplex virus type 1 latency-associated transcript (LAT) enhancer/rcr is hyperacetylated during latency independently of LAT transcription. *Journal of Virology*, *78* (22), 12508–12518. doi:10.1128/JVI.78.22.12508-12518.2004
- Kulu, Y., Dorfman, J. D., Kuruppu, D., Fuchs, B. C., Goodwin, J. M., Fujii, T., Kuroda, T., Lanuti, M., & Tanabe, K. K. (2009). Comparison of intravenous versus intraperitoneal administration of oncolytic herpes simplex virus 1 for peritoneal carcinomatosis in mice. *Cancer Gene Therapy*, *16* (4), 291–297. doi:10.1038/cgt.2008.83
- Kumar, D. K., Eimer, W. A., Tanzi, R. E., & Moir, R. D. (2016). Alzheimer's disease: The potential therapeutic role of the natural antibiotic amyloid-beta peptide. *Neurodegenerative Disease Management*, *6* (5), 345–348. doi:10.2217/nmt-2016-0035
- Lanfranco, M. F., Mochetti, I., Burns, M. P., & Villapol, S. (2018). Glial- and neuronal-specific expression of CCL5 mRNA in the Rat brain. *Frontiers in Neuroanatomy*, *11*, 137. doi:10.3389/fnana.2017.00137
- Li, L., Li, Y., Li, X., Xia, Y., Wang, E., Gong, D., Chen, G., Yang, L., Zhang, K., Zhao, Z., Fraser, N. W., Fan, Q., Li, B., Zhang, H., Cao, X., & Zhou, J. (2020). HSV-1 infection and pathogenesis in the tree shrew eye following corneal inoculation. *Journal of Neurovirology*, *26* (3), 391–403.
- Liu, Y. T., Jih, J., Dai, X., Bi, G. Q., & Zhou, Z. H. (2019). Cryo-EM structures of herpes simplex virus type 1 portal vertex and packaged genome. *Nature*, *570* (7760), 257–261. doi:10.1038/s41586-019-1248-6
- Marcocci, M. E., Napoletani, G., Protto, V., Kolesova, O., Piacentini, R., Li Puma, D. D., Lomonte, P., Grassi, C., Palamara, A. T., & De Chiara, G. (2020). Herpes simplex virus-1 in the brain: The dark side of a sneaky infection. *Trends in Microbiology*, *28* (10), 808–820.
- McManus, R. M., & Heneka, M. T. (2017). Role of neuroinflammation in neurodegeneration: New insights. *Alzheimer's Research & Therapy*, *9* (1), 14. doi:10.1186/s13195-017-0241-2
- McQuillan, G., Kruszon-Moran, D., Flagg, E. W., & Paulose-Ram, R. (2018). *Prevalence of Herpes Simplex Virus Type 1 and Type 2 in Persons Aged 14–49: United States, 2015–2016*. NCHS Data Brief No. 304. 2018 Feb, (304), 1-8. <https://www.cdc.gov/nchs/products/databriefs/db304.htm>
- Mehta, A., Maggioncalda, J., Bagasra, O., Thikkavarapu, S., Saikumari, P., Valyi-Nagy, T., Fraser, N. W., & Block, T. M. (1995). In situ DNA PCR and RNA hybridization detection of herpes simplex virus sequences in trigeminal ganglia of latently infected mice. *Virology*, *206* (1), 633–640. doi:10.1016/s0042-6822(95)80080-8
- Menendez, C. M., & Carr, D. J. J. (2017). Herpes simplex virus-1 infects the olfactory bulb shortly following ocular infection and

- exhibits a long-term inflammatory profile in the form of effector and HSV-1-specific T cells. *Journal of Neuroinflammation*, *14* (1), 124. doi:10.1186/s12974-017-0903-9
- Menendez, C. M., Jinkins, J. K., & Carr, D. J. (2016). Resident T cells are unable to control herpes simplex virus-1 activity in the brain ependymal region during latency. *Journal of Immunology*, *197* (4), 1262–1275. doi:10.4049/jimmunol.1600207
- Michaelis, K. A., Norgard, M. A., Levasseur, P. R., Olson, B., Burfeind, K. G., Buenafe, A. C., Zhu, X., Jeng, S., McWeeney, S. K., & Marks, D. L. (2019). Persistent toll-like receptor 7 stimulation induces behavioral and molecular innate immune tolerance. *Brain Behavior and Immunity*, *82*, 338–353. doi:10.1016/j.bbi.2019.09.004
- Nicoll, M. P., Hann, W., Shivkumar, M., Harman, L. E., Connor, V., Coleman, H. M., Proenca, J. T., & Efstathiou, S. (2016). The HSV-1 latency-associated transcript functions to repress latent phase lytic gene expression and suppress virus reactivation from latently infected neurons. *PLoS Pathogens*, *12* (4), e1005539. doi:10.1371/journal.ppat.1005539
- Nicoll, M. P., Proenca, J. T., & Efstathiou, S. (2012). The molecular basis of herpes simplex virus latency. *FEMS Microbiology Reviews*, *36* (3), 684–705. doi:10.1111/j.1574-6976.2011.00320.x
- Pluinage, J. V., Haney, M. S., Smith, B. A. H., Sun, J., Iram, T., Bonanno, L., Li, L., Lee, D. P., Morgens, D. W., Yang, A. C., Shuken, S. R., Gate, D., Scott, M., Khatri, P., Luo, J., Bertozzi, C. R., Bassik, M. C., & Wyss-Coray, T. (2019). CD22 Blockade restores homeostatic microglial phagocytosis in ageing brains. *Nature*, *568* (7751), 187–192. doi:10.1038/s41586-019-1088-4
- Readhead, B., Haure-Mirande, J.-V., Funk, C. C., Richards, M. A., Shannon, P., Haroutunian, V., Sano, M., Liang, W. S., Beckmann, N. D., Price, N. D., Reiman, E. M., Schadt, E. E., Ehrlich, M. E., Gandy, S., & Dudley, J. T. (2018). Multiscale analysis of independent Alzheimer's cohorts finds disruption of molecular, genetic, and clinical networks by human herpesvirus. *Neuron*, *99* (1), 64–82.e7. doi:10.1016/j.neuron.2018.05.023
- Reil, H., Bartlime, A., Drerup, J., Grewing, T., & Korn, K. (2008). Clinical validation of a new triplex real-time polymerase chain reaction assay for the detection and discrimination of herpes simplex virus types 1 and 2. *The Journal of Molecular Diagnostics*, *10* (4), 361–367.
- Rock, D. L., & Fraser, N. W. (1983). Detection of HSV-1 genome in central nervous system of latently infected mice. *Nature*, *302* (5908), 523–525.
- Roussarie, J. P., Yao, V., Rodriguez-Rodriguez, P., Oughtred, R., Rust, J., Plautz, Z., Kasturia, S., Albornoz, C., Wang, W., Schmidt, E. F., Dannenfelser, R., Tadych, A., Brichta, L., Barnea-Cramer, A., Heintz, N., Hof, P. R., Heiman, M., Dolinski, K., Flajolet, M., ..., & Greengard, P. (2020). Selective neuronal vulnerability in Alzheimer's disease: A network-based analysis. *Neuron*, *107* (5), 821–835 e812. doi:10.1016/j.neuron.2020.06.010
- Sait, A., Angeli, C., Doig, A. J., & Day, P. J. R. (2021). Viral involvement in Alzheimer's disease. *ACS Chemical Neuroscience*, *12* (7), 1049–1060. doi:10.1021/acscchemneuro.0c00719
- Sala Frigerio, C., Wolfs, L., Fattorelli, N., Thrupp, N., Voytyuk, I., Schmidt, I., Mancuso, R., Chen, W. T., Woodbury, M. E., Srivastava, G., Moller, T., Hudry, E., Das, S., Saido, T., Karran, E., Hyman, B., Perry, V. H., Fiers, M., & De Strooper, B. (2019). The Major risk factors for Alzheimer's disease: Age, sex, and genes modulate the microglia response to abeta plaques. *Cell Reports*, *27* (4), 1293–1306.e1296. doi:10.1016/j.celrep.2019.03.099
- Santana, S., Recuero, M., Bullido, M. J., Valdivieso, F., & Aldudo, J. (2012). Herpes simplex virus type I induces the accumulation of intracellular β -amyloid in autophagic compartments and the inhibition of the non-amyloidogenic pathway in human neuroblastoma cells. *Neurobiology of Aging*, *33* (430), e419–430.e433. doi:10.1016/j.neurobiolaging.2010.12.010
- Tong, Y., McCarthy, K., Kong, H., & Lemieux, B. (2012). Development and comparison of a rapid isothermal nucleic acid amplification test for typing of herpes simplex virus types 1 and 2 on a portable fluorescence detector. *The Journal of Molecular Diagnostics*, *14* (6), 569–576. doi:10.1016/j.jmoldx.2012.05.005
- Ukpo, O. C., Flanagan, J. J., Ma, X. J., Luo, Y., Thorstad, W. L., & Lewis, J. S., Jr. (2011). High-risk human papillomavirus E6/E7 mRNA detection by a novel in situ hybridization assay strongly correlates with p16 expression and patient outcomes in oropharyngeal squamous cell carcinoma. *American Journal of Surgical Pathology*, *35* (9), 1343–1350. doi:10.1097/PAS.0b013e318220e59d
- Wang, F., Flanagan, J., Su, N., Wang, L. C., Bui, S., Nielson, A., Wu, X., Vo, H. T., Ma, X. J., & Luo, Y. (2012). RNAscope: A novel in situ RNA analysis platform for formalin-fixed, paraffin-embedded tissues. *The Journal of Molecular Diagnostics*, *14* (1), 22–29. doi:10.1016/j.jmoldx.2011.08.002
- Wilson, A. C., & Mohr, I. (2012). A cultured affair: HSV latency and reactivation in neurons. *Trends in Microbiology*, *20* (12), 604–611. doi:10.1016/j.tim.2012.08.005
- Xu, F., Schillinger, J. A., Sternberg, M. R., Johnson, R. E., Lee, F. K., Nahmias, A. J., & Markowitz, L. E. (2002). Seroprevalence and coinfection with herpes simplex virus type 1 and type 2 in the United States, 1988–1994. *Journal of Infectious Diseases*, *185* (8), 1019–1024. doi:10.1086/340041
- Yao, H. W., Ling, P., Tung, Y. Y., Hsu, S. M., & Chen, S. H. (2014). In vivo reactivation of latent herpes simplex virus 1 in mice can occur in the brain before occurring in the trigeminal ganglion. *Journal of Virology*, *88* (19), 11264–11270. doi:10.1128/JVI.01616-14
- Zhang, J., Zhao, J., Li, J., Xu, S., He, S., Zeng, Y., Xie, L., Xie, N., Liu, T., Lee, K., Seo, G. J., Chen, L., Stabell, A. C., Xia, Z., Sawyer, S. L., Jung, J., Huang, C., & Feng, P. (2018). Species-specific deamidation of cGAS facilitates herpes simplex virus lytic replication. *Cell Host & Microbe*, *24* (2), 234–248.e5. doi:10.1016/j.chom.2018.07.004